

## Recharging processes of Cr ions in $\text{Mg}_2\text{SiO}_4$ and $\text{Y}_3\text{Al}_5\text{O}_{12}$ crystals under influence of annealing and $\gamma$ - irradiation

S. M. Kaczmarek\*<sup>1</sup>, W. Chen<sup>2</sup>, and G. Boulon<sup>2</sup>

<sup>1</sup> Institute of Physics, Szczecin University of Technology, Al. Piastów 48, 70-310 Szczecin, Poland

<sup>2</sup> Physical Chemistry of Luminescent Materials, Claude Bernard /Lyon 1 University, UMR CNRS 5620, Bat. A. Kastler, 10 rue Ampère, 69622 Villeurbanne, France

Received 21 December 2004, accepted 18 March 2005

Published online 15 December 2005

**Key words** chromium, forsterite, yttrium aluminum garnet, annealing,  $\gamma$ -irradiation, photoluminescence.

**PACS** 61.72.Ji, 61.80.Ed, 42.70.Ij

Recharging processes of chromium ions were investigated for  $\text{Mg}_2\text{SiO}_4$ :Mg, Cr single crystals using annealing in  $\text{O}_2$  and in air and  $\gamma$ -irradiation, as compare to YAG:Ca, Cr single crystals. The formation of tetravalent Cr ions in the  $\text{Mg}_2\text{SiO}_4$ :Mg, Cr is related not only to the initial Cr content in the melt, oxygen partial pressure and  $\text{O}^{2-}$  vacancy existing in the crystal, but also to the external field such as  $\gamma$ -irradiation. The additional absorption after  $\gamma$ -irradiation shows the decrease in intensity of the absorption of  $\text{Cr}^{3+}$  and  $\text{Cr}^{4+}$  ions in some part of the spectrum and increase in the other giving evidence on recharging effects between  $\text{Cr}^{3+}$  and  $\text{Cr}^{4+}$ . There arises also color centers observed between 380 nm and 570 nm that may participate in energy transfer of any excitation to  $\text{Cr}^{4+}$  giving rise to  $\text{Cr}^{4+}$  emission. Opposite to forsterite crystal, absorption spectrum of YAG:Ca, Cr crystal after  $\gamma$ -irradiation reveals only increase in the absorption of the Cr bands. The observed behavior of the absorption spectrum of YAG:Ca, Cr crystal under influence of  $\gamma$ -irradiation suggests that  $\gamma$ -irradiation ionizes only Cr ions.

© 2006 WILEY-VCH Verlag GmbH & Co. KGaA, Weinheim

### 1 Introduction

Since the demonstration of forsterite:Cr laser [1,2], remarkable progress has been made in the development of forsterite:Cr lasers with high performance. For example, an all-solid-state forsterite:Cr laser generated 14-fs pulses at 1.3  $\mu\text{m}$  with 80 mW average power at 100 MHz repetition rate [3].

To optimize the performance of a Cr:forsterite laser, it is necessary to seek a balance between laser gain and optical losses. A shorter forsterite:Cr crystal with an enough high  $\text{Cr}^{4+}$  concentration will decrease its optical losses, and will introduce less group velocity dispersion and beam astigmatism, which is useful for the ultrafast lasers [4].

The difficulties to grow a high concentration forsterite:Cr crystal with laser quality include not only the doping of high content Cr, but also the valence control of  $\text{Cr}^{4+}$  laser center. To increase the concentration of tetravalent  $\text{Cr}^{4+}$  in forsterite:Cr, it seems required to apply a high Cr doping content and a high oxygen partial pressure [5]. The formation of tetravalent  $\text{Cr}^{4+}$  is related also to the concentration of an oxygen vacancy existing in the crystallized forsterite:Cr [6,7]. In the paper a set of defect reaction formulas concerning the formation of tetravalent  $\text{Cr}^{4+}$  in forsterite:Cr were established on the basis of the experimental results of growth and annealing. It was found that an oxygen vacancy existing in forsterite:Cr was most probably a critical factor to form tetravalent  $\text{Cr}^{4+}$  and to make its concentration (i.e., the near-infrared absorption intensity) gradually saturated. It was proved that an as-grown forsterite:Cr crystal with such an oxygen vacancy could possess much higher  $\text{Cr}^{4+}$  absorption intensity in the near-infrared wavelength range after an oxidation annealing.

\* Corresponding author: e-mail: skaczmarek@ps.pl

Kück et al. and Henderson et al. [8,9] have performed optical spectroscopy measurements and optimal crystal growth experiments of some Cr<sup>4+</sup>-doped garnets. Kaczmarek and Zendzian et al. [10] have proved useful experiments giving rise in the laser efficiency of YAG:Cr, Tm, Ho crystal after annealing and subsequent irradiation with  $\gamma$ -quanta. In the present letter a set of experiments were performed on the influence of  $\gamma$ -irradiation on the absorption spectrum in the UV-VIS and emission intensity of forsterite:Cr crystal as compare to yttrium aluminum garnet:Cr one in the infrared region.

## 2 Experimental

High concentration forsterite:Cr (Mg<sub>2</sub>SiO<sub>4</sub>:Cr) laser crystals were grown out successfully by a medium-frequency induction-heating Czochralski method in an atmosphere containing oxygen in the Physical Chemistry of Luminescent Materials, Lyon, France. MgO-rich, nonstoichiometric mixtures of high purity MgO, SiO<sub>2</sub> and Cr<sub>2</sub>O<sub>3</sub> powders were used at growth run, in which the initial Cr content in the mixtures was about 0.6%. Cr:forsterite crystal reported here was grown along *a*-axis.

A special design for the temperature field was made to maintain enough Marangoni thermal convection, which is caused by a surface tension gradient as a result of the temperature gradient near the surface of the melt. Large dimension (35–38 mm diameter  $\times$  90–110 mm length) forsterite:Cr crystals with variant Cr<sup>4+</sup> concentrations (the absorption coefficient at 1064 nm = 0.3–3.0 cm<sup>-1</sup>) were grown out successfully. The colour of as-grown forsterite:Cr crystal rods looks like pale or dark blue, depending on initial Cr doping content. Annealing of the crystal in O<sub>2</sub> was performed at 1373 °K giving dark blue crystal. Cylindrical samples were cut from the oriented forsterite:Cr rods and polished on all faces (polished faces were *a*-faces). The yttrium-aluminum garnet single crystals co-doped with Cr (1 at. %) and Ca have been grown by the Czochralski method along [111] direction in the nitrogen atmosphere with addition of 3 vol. % of oxygen. The colors of as grown crystal and annealed in the air one were of black. The samples were prepared as plates with diameter of about 10 mm and thickness of about 1 mm cut perpendicularly to growth axis.

The annealed sample was underwent to  $\gamma$ -irradiation in the Institute of Nuclear Chemistry and Technology, Warsaw with a dose of 10<sup>5</sup> Gy. The color of the forsterite:Cr crystal changed to blue-green while yttrium aluminum garnet:Cr to brown one. Room-temperature absorption spectra were measured before and after  $\gamma$ -irradiation by a Perkin–Elmer Lambda 900 spectrometer. The additional absorption coefficient after gamma irradiation of a given sample was calculated from the following equation:

$$\Delta K = \frac{1}{d} \ln \frac{T_1}{T_2}, \quad (1)$$

where *d* denotes the sample thickness, and *T*<sub>1</sub> and *T*<sub>2</sub> are transmissions of the sample before and after a given treatment. Photoluminescence measurements were carried out for annealed in oxygen and  $\gamma$ -irradiated crystals using a SS-900 Edinburgh Inc. spectrophotometer in the Institute of Optoelectronics, MUT, Poland.

## 3 Results

Annealed in O<sub>2</sub> Mg<sub>2</sub>SiO<sub>4</sub>:Mg, Cr (0.6wt.%) (polarization *E*//*b*) crystal (Fig. 1, curve 1) reveals fundamental absorption edge at 240 nm and sharp lattice absorption band at 5000 nm, moreover the following absorption bands are distinguishable: 360 nm, 430 nm, 550 nm, 630 nm, 660 nm, 705 nm, 725 nm, 800 nm, 986 nm and 1055 nm. As compare to “as-grown” crystal in the absorption spectrum of the annealed in O<sub>2</sub> crystal one can observe the bleaching of the crystal in the range of wavelengths up to 600 nm and positive additional absorption bands for wavelengths: 600–750 nm and 900–1150 nm, and, negative one, centered at about 750 nm. The bands suggest recharging of Cr ions. The first band seem to be mixed Cr<sup>3+</sup>-Cr<sup>4+</sup> band, the second band may be assigned to mixed Cr<sup>4+</sup>-Cr<sup>5+</sup> band, while the third one seem to be the effect of Cr<sup>4+</sup> ionization.

In the absorption spectrum of the crystal underwent to gamma irradiation with a dose of 10<sup>5</sup> Gy one can observe (Fig. 1, curve 2) some shifting of the fundamental absorption edge (a band centered at about 275 nm that intensity strongly depend on the dose of  $\gamma$ -irradiation, seen for curve 3). Moreover we observed the following additional bands with respect to annealed only crystal: 380 nm, 460 nm and 570 nm sharp small band. Beside the bands we observed an increase of the absorption of the following bands present in annealed crystal: 550 nm, 705 nm, 740 nm and the decrease in the absorption of the following bands: 630 nm (Cr<sup>3+</sup>), 660

nm ( $\text{Cr}^{4+}$ ), 986 nm ( $\text{Cr}^{4+}$ ) and 1055 nm ( $\text{Cr}^{4+}$ ). It means that under influence of  $\gamma$ -irradiation recharging processes take place between  $\text{Cr}^{3+}$  and  $\text{Cr}^{4+}$  and  $\text{Cr}^{6+}$  ions.

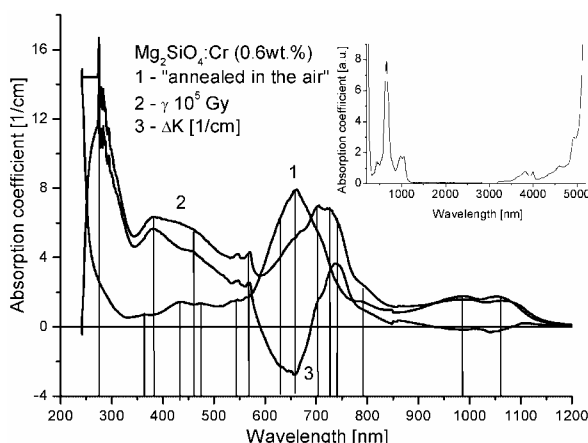


**Fig. 1** Absorption of annealed in  $\text{O}_2$  (1),  $\gamma$ -irradiated with a dose of  $10^5$  Gy (2) and additional absorption after the  $\gamma$ -irradiation of  $\text{Mg}_2\text{SiO}_4:\text{Mg}, \text{Cr}$  (0.6wt.%) single crystal.

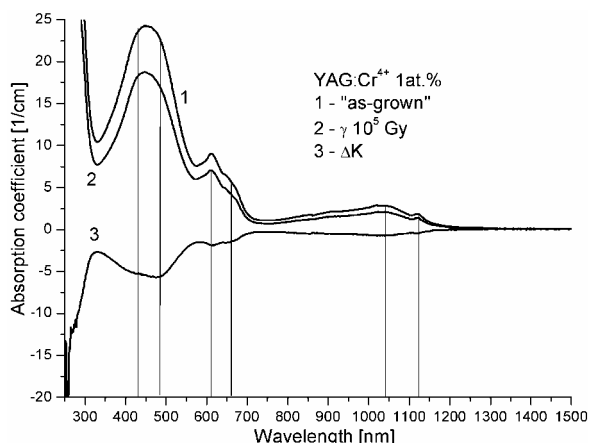


**Fig. 2** Absorption of “as-grown” (1),  $\gamma$ -irradiated with a dose of  $10^5$  Gy (2) and additional absorption after the  $\gamma$ -irradiation of  $\text{YAG}:\text{Ca}, \text{Cr}$  (1wt.%) (3) single crystal.

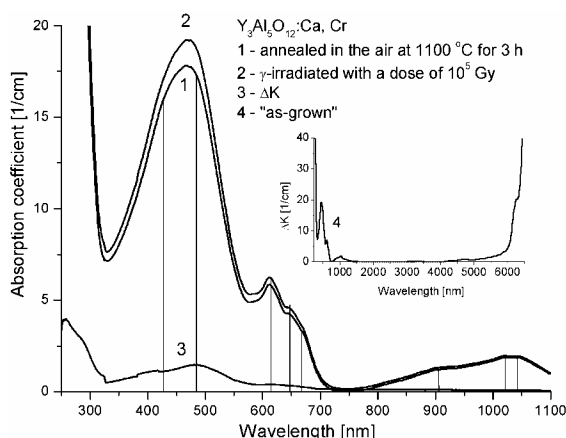


**Fig. 2a** Absorption of annealed in the air at  $1100^\circ\text{C}$  for 3h (1),  $\gamma$ -irradiated with a dose of  $10^5$  Gy (2) and additional absorption after the  $\gamma$ -irradiation of  $\text{YAG}:\text{Ca}, \text{Cr}$  (1wt.%) (3) single crystal. In the inset the absorption of “as-grown” crystal in optical window is present (4).

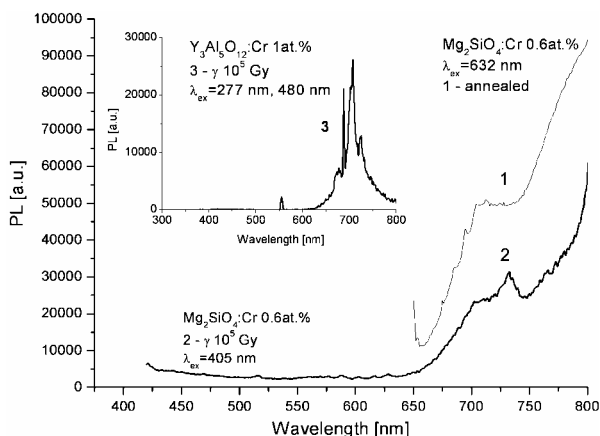


**Fig. 3** Photoluminescence spectra for annealed in  $\text{O}_2$  (1) and for  $\gamma$ -irradiated (2) forsterite crystal. In the inset PL spectrum of  $\text{Y}_3\text{Al}_5\text{O}_{12}:\text{Cr}$  (1at.%) crystal is presented.

In fig. 2 we show similar results for “as-grown”  $\text{YAG}:\text{Ca}, \text{Cr}^{4+}$  (1wt.%) crystal, where simultaneous presence of  $\text{Cr}^{3+}$  and  $\text{Cr}^{4+}$  ions we found. Fundamental absorption starts at 248 nm, lattice one at 6200 nm. The following absorption bands one can distinguish for both “as-grown” and  $\gamma$ -irradiated with a dose of  $10^5$  Gy crystal: 430 nm (assigned, as previously, to  ${}^4\text{A}_2 \rightarrow {}^4\text{T}_1$  transition), 475 nm ( $\text{Cr}^{4+}$ ), 613 nm (assigned to  ${}^4\text{A}_2 \rightarrow {}^4\text{T}_2$  transition of  $\text{Cr}^{3+}$ ), 660 nm ( $\text{Cr}^{4+}$ ), 1040 nm ( $\text{Cr}^{4+}$ ) and 1125 nm ( $\text{Cr}^{4+}$ ). After  $\gamma$ -irradiation negative absorption bands arises in the additional absorption spectrum with the same positions of absorption peaks as in the case of the absorption.

In fig. 2a similar results for  $\text{YAG}:\text{Ca}, \text{Cr}^{4+}$  (1wt.%) annealed in the air for 3h at  $1100^\circ\text{C}$  and subsequently  $\gamma$ -irradiated are presented. The following absorption bands one can distinguish: 430 nm (assigned, as previously, to  ${}^4\text{A}_2 \rightarrow {}^4\text{T}_1$  transition), 475 nm ( $\text{Cr}^{4+}$ ), 613 nm (assigned to  ${}^4\text{A}_2 \rightarrow {}^4\text{T}_2$  transition of  $\text{Cr}^{3+}$ ), 660 nm ( $\text{Cr}^{4+}$ ), 905 nm, 1025 nm (probably  $\text{Cr}^{5+}$ ), and 1040 nm ( $\text{Cr}^{4+}$ ). In the inset the absorption of “as-grown” crystal in the range of optical window one can observe. After  $\gamma$ -irradiation the following bands arises in the additional absorption spectrum: 260 nm, 475 nm, 613 nm, 660 nm and wide, un-structural band over 700 nm. Fig. 3

presents PL spectra for annealed in  $O_2$  (1) and  $\gamma$ -irradiated (2)  $Mg_2SiO_4:Mg, Cr$  single crystal. As one can see excitations with 632 nm and 405 nm, respectively, lead to arising of 725 nm centered usual emission of  $Cr^{3+}$  ions. The emission is weaker one then emission of  $Cr^{4+}$  ions. Moreover, in the inset one can see clear  $Cr^{3+}$  emission of  $\gamma$ -irradiated YAG:Ca,  $Cr^{4+}$  crystal.

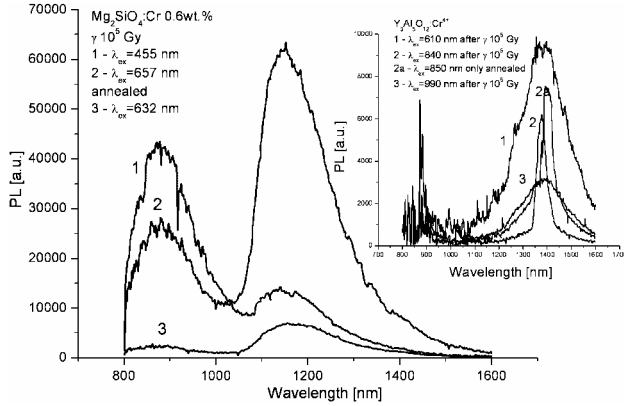


**Fig. 4** Photoluminescence of annealed in  $O_2$   $Mg_2SiO_4:Cr$  crystal excited with 632 nm (curve 3) and  $\gamma$ -irradiated one excited with 455 nm (curve 1) and 657 nm (curve 2). In the inset PL of  $\gamma$ -irradiated as compare to annealed crystal are presented.

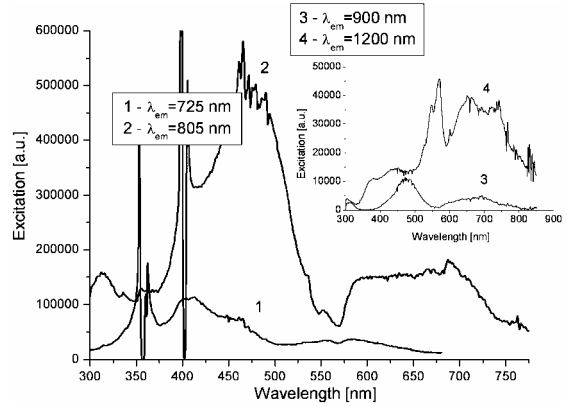


**Fig. 5** Excitation spectra of annealed in  $O_2$   $Mg_2SiO_4:Cr$  crystal for  $\lambda_{em}=725$  nm (curve 1), 805 nm (curve 2), 900 nm (curve 3) and 1200 nm (curve 4).

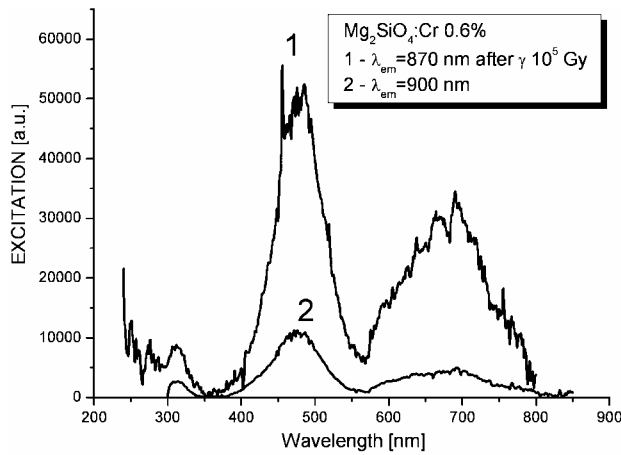


**Fig. 6** Excitation spectra for annealed in  $O_2$  (curve 2, 900 nm emission) and  $\gamma$ -irradiated  $Mg_2SiO_4:Cr$  crystal (curve 1, 870 nm emission).

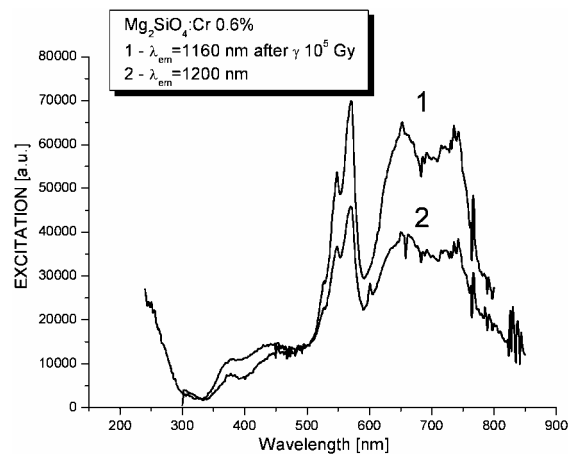


**Fig. 7** Excitation spectra for annealed in  $O_2$  (curve 2, 1200 nm emission) and  $\gamma$ -irradiated  $Mg_2SiO_4:Cr$  crystal (curve 1, 1160 nm emission).

In fig. 4 there are presented PL curves for both: annealed in  $O_2$  (curve 3 – 632 nm excitation) and  $\gamma$ -irradiated (curve 1 – 455 nm excitation and curve 2 – 657 nm excitation)  $Mg_2SiO_4$  single crystal. In the inset of the figure PL curves are presented for annealed in the air (curve 2a,  $\lambda_{ex} = 850$  nm) and  $\gamma$ -irradiated YAG:Ca,  $Cr^{4+}$  (curves 1-3,  $\lambda_{ex}=610$  nm, 840 nm and 990 nm, respectively) crystal. In fig. 5 we presented excitation curves for  $Mg_2SiO_4:Cr$  crystal annealed in  $O_2$ . In Figs 6 and 7 one can see the influence of  $\gamma$ -irradiation on the  $Cr^{3+}$  and  $Cr^{4+}$  excitations bands.

## 4 Discussion

Forsterite, a member of the olivine family, has an orthorhombic lattice structure with space group  $P_{bmm}$  ( $a=4.76$  Å,  $b=10.22$  Å,  $c=5.99$  Å). In the lattice,  $Mg^{2+}$  ions ( $R_{CN=6}=0.72$  Å [11]) are in two crystallographic distinct

positions,  $4a$  and  $4c$ , which have inversion and mirror point symmetry, respectively.  $\text{Si}^{4+}$  ions ( $R_{\text{CN}=6}=0.26 \text{ \AA}$  [11]) are in  $4c$  position with mirror point symmetry. The  $\text{Si}^{4+}$  tetrahedron connects with two types of  $\text{Mg}^{2+}$  octahedrons. In the  $\text{Mg}_2\text{SiO}_4:\text{Mg, Cr}$  crystal, most of Cr ions appear as trivalent  $\text{Cr}^{3+}$  and a small part of Cr ions appear as tetravalent  $\text{Cr}^{4+}$ . The doping of trivalent  $\text{Cr}^{3+}$  is mainly limited by its segregation coefficient. The formation of tetravalent  $\text{Cr}^{4+}$  is related not only to the initial Cr content in the melt and the oxygen partial pressure in the growth chamber, but also most probably to the concentration of an oxygen vacancy existing in the crystallized forsterite:Cr.

In the case of forsterite:Cr, although there is larger difference between the ionic radii of the substitution and host cations, the initial symmetry of the host cations is the main argument for the substitution of  $\text{Cr}^{4+}$  ( $R_{\text{CN}=4}=0.44 \text{ \AA}$  [11]) of  $3d^2$  configuration in tetrahedral  $\text{Si}^{4+}$  site (1055 nm band observed in our experiments), and the substitution of  $\text{Cr}^{3+}$  ( $R_{\text{CN}=6}=0.615 \text{ \AA}$  [11]) of  $3d^3$  configuration in octahedral  $\text{Mg}^{2+}$  sites (430 nm band observed in our experiment) [1, 12]. Besides, there is another possibility to find  $\text{Cr}^{4+}$  ions ( $R_{\text{CN}=6}=0.55 \text{ \AA}$  [11]) in the two octahedral  $\text{Mg}^{2+}$  sites ( $R_{\text{CN}=6}=0.72 \text{ \AA}$  [11]) instead of the smaller tetrahedral  $\text{Si}^{4+}$  ions, as discussed for YAG:Cr, Ca crystal. They may be 550 nm, 660 nm and wide 700–800 nm band. Other possibilities have also to be considered:  $\text{Cr}^{5+}$  ( $R_{\text{CN}=4}=0.35 \text{ \AA}$  [11]) of  $3d^1$  configuration and  $\text{Cr}^{6+}$  ( $R_{\text{CN}=4}=0.30 \text{ \AA}$  [11]) of  $3d^0$  configuration in the tetrahedral site of  $\text{Si}^{4+}$  ( $R_{\text{CN}=4}=0.26 \text{ \AA}$  [11]), which probably occur during oxidation processes and are characterized by a closer ionic radius than  $\text{Cr}^{4+}$ . If  $\text{Cr}^{3+}$  and  $\text{Cr}^{4+}$  absorption and emission spectra are well recognized in the visible and near-infrared range, those of  $\text{Cr}^{5+}$  are probably observed by an absorption broad band near 950–1000 nm and an emission broad band near 1300 nm in the similar range as  $\text{Cr}^{4+}$ , as shown in  $\text{ZrSiO}_4$  [13] and  $\text{YVO}_4$ ,  $\text{YPO}_4$  and apatites [14]. These two kinds of ions can be distinguished by lifetime values, in the  $\mu\text{s}$  scale for  $\text{Cr}^{4+}$  and the hundred-ns scale for  $\text{Cr}^{5+}$ .  $\text{Cr}^{6+}$  is only probably observed by an UV absorption broad band between 350 and 400 nm [7].

Among the bands we observed in the room absorption spectrum (Fig. 1) the 360 nm band is probably assigned to  $3d^0$  configuration of  $\text{Cr}^{6+}$ , 430 nm is assigned to  ${}^4\text{A}_2 \rightarrow {}^4\text{T}_1$  transition of  $\text{Cr}^{3+}$  ions located at  $\text{Mg}^{2+}$  ( $4c$  sites), 550 nm to  $\text{Cr}^{4+}$  site (may be one of octahedral  $\text{Mg}^{2+}$  sites), 630 nm to  ${}^4\text{A}_2 \rightarrow {}^4\text{T}_2$  transition of  $\text{Cr}^{3+}$ , 660 nm to  $\text{Cr}^{4+}$  site (may be one of octahedral  $\text{Mg}^{2+}$  sites), 705 nm, 725 nm, 800 nm, 986 nm ( $\text{Cr}^{4+}$  and  $\text{Cr}^{5+}$  sites) and 1055 nm to  ${}^3\text{A}_2 \rightarrow {}^3\text{A}_1({}^3\text{T}_2)$  transition of tetravalent Cr ions located at  $\text{Si}^{4+}$  sites). If there would be not energy transfer between  $\text{Cr}^{3+}$  and  $\text{Cr}^{4+}$  sites it could be possible to separate the sites (550 nm, 660 nm and 700–800 nm) giving full information on its origin using e.g. Site Selective Laser Spectroscopy Method. Because the energy transfer between Cr ions is rather expected, we can not separate the sites and will stay with supposition on  $\text{Cr}^{4+}$  origin of the absorption.

The general property of oxides to which forsterite and YAG belong is oxygen vacancy formation due to vacuum annealing (or annealing in inert gas atmosphere) [6,8,9]. In the absorption spectrum of  $\gamma$ -irradiated forsterite crystal we observe 275 nm additional band that may be interpreted as a valence change of  $\text{Si}^{4+}$  ions due to capture of electron coming from ionization of  $\text{O}^{2-}$  ion. The same phenomenon we observed for  $\text{SrLaGa}_3\text{O}_7$  single crystals [15], where for  $\text{GaO}_4$  tetrahedra we observed the following process:  $\text{Ga}^{3+}$  ion captures the electron which was knocked out from  $\text{O}^{2-}$  ion by  $\gamma$  irradiation and in a consequence,  $\text{Ga}^{2+}$  paramagnetic center is formed. In our case  $\text{Si}^{3+}$  ion arises in the same consequence.

380 nm additional absorption band is assigned probably to  $\text{Cr}^{6+}$  ions of  $3d^0$  configuration or more probably to  $\text{O}^-$  hole centers and/or F-centers [16]. The hole centers are formed due to electron photoionization from the valence to the conduction band in crystals when the concentration of oxygen vacancies is negligible (oxidization). We think in our crystals even after oxidization process there exist some amount of oxygen vacancies. So the 380 nm band should be rather assigned to F-centers. 460 nm and/or 570 nm bands may be assigned to  $\text{F}^+$  color centers. The 380–570 nm wide color center band may participate in energy transfer to  $\text{Cr}^{4+}$  giving rise of  $\text{Cr}^{4+}$  emission observed in photoluminescence characteristics.

Opposite to forsterite crystal, absorption spectrum of YAG:Ca, Cr “as-grown” crystal (Fig. 2) after  $\gamma$ -irradiation reveals only decrease in the absorption of the Cr bands [17]. The observed behavior of the absorption spectrum (negative additional absorption) of YAG:Ca, Cr “as-grown” crystal under influence of  $\gamma$ -irradiation suggests that  $\gamma$ -irradiation reduce only Cr ions by incorporation of Compton electrons. It is confirmed by photoluminescence measurements and previously observed analogical changes taking place in the crystal under annealing in hydrogen [17,9].

Annealed in the air YAG:Ca, Cr crystal (Fig. 2a) reveals the presence of something different absorption bands as compare to “as-grown” crystal [8,9]. Due to annealing in the air new bands arises: 905 nm and 1025 nm, assigned probably to  $\text{Cr}^{5+}$  ions. There is missed also 1125 nm band assigned to  $\text{Cr}^{4+}$ . As compare to “as-

grown”, annealed in the air YAG:Ca, Cr crystal after  $\gamma$ -irradiation shows some completely different changes. There arises additional absorption bands in the ranges of  $\text{Cr}^{4+}$  absorption that allow to give supposition on ionizing influence of  $\gamma$ -quanta on the crystal. The band peaked at 260 nm may be assigned to  $\text{Fe}^{3+}$  ions (created by ionization of  $\text{Fe}^{2+}$ ) of which unintentionally doped is the crystal. Other bands are simply  $\text{Cr}^{4+}$  bands created by ionization of  $\text{Cr}^{3+}$ . There are missed color centers that were seen in the additional absorption of annealed in  $\text{O}_2$   $\text{Mg}_2\text{SiO}_4:\text{Mg}$ , Cr crystal.

Photoluminescence curves of  $\text{O}_2$  annealed  $\text{Mg}_2\text{SiO}_4:\text{Mg}$ , Cr crystal reveal the presence of  $\text{Cr}^{3+}$  ions but the intensity of the  $\text{Cr}^{3+}$  ions centered at about 725 nm is much lower than intensity of the  $\text{Cr}^{4+}$  ones. It may give evidence on  $\text{Cr}^{3+}$  to  $\text{Cr}^{4+}$  energy transfer. As it results from fig. 1  $\text{Cr}^{3+}$  and  $\text{Cr}^{4+}$  absorption bands (see 550 – 800 nm range of the absorption spectrum) are closely placed each to other, so, non-radiative transitions of excited electrons are very probably between the bands.

By comparing curves 2 and 3 of fig. 4 one can state that  $\gamma$ -irradiation leads to increase in the amount of  $\text{Cr}^{4+}$  emitting centers. Moreover there is seen a difference in different types of  $\text{Cr}^{4+}$  centers excited with 455 nm (strongest emission peaked at about 900 nm) and with 657 nm (strongest emission peaked at about 1150 nm).

As one can see from fig. 5 usual  $\text{Cr}^{3+}$  emission (725 nm band) one can obtain with 430 nm excitation but there is a band overlapping with  $\text{Cr}^{4+}$  (805 nm) emission (475 nm absorption band) due to which energy transfer take place between  $\text{Cr}^{3+}$  and  $\text{Cr}^{4+}$  ions. 900 nm  $\text{Cr}^{4+}$  emission is excited by 475 nm absorption band and a wide 600-800 nm absorption band assigned both to  $\text{Cr}^{3+}$  and  $\text{Cr}^{4+}$  ions. 1200 nm emission is excited by two main absorption bands:  $\text{Cr}^{4+}$  absorption centered at about 550 nm and  $\text{Cr}^{4+}$  absorption centered about 700 nm. Both 550 nm and 700 nm absorption bands come from different  $\text{Cr}^{4+}$  centers.

From fig. 6 it results the emission peaked at about 900 nm is due to excitation of  $\text{Cr}^{3+}$  and  $\text{Cr}^{4+}$  ions and energy transfer between them. The  $\gamma$ -irradiation leads to increase in intensity of excitation spectra. The same phenomenon should be observed for emission spectra as can be observed in fig. 4. From fig. 7 one can see the same character of changes of the excitation spectrum for 1200 nm emission under influence of  $\gamma$ -irradiation as previously for 900 nm emission. So, we can state, in the case of forsterite  $\text{Mg}_2\text{SiO}_4:\text{Mg}$ , Cr single crystal  $\gamma$ -irradiation leads to increase in the amount of  $\text{Cr}^{4+}$  luminescence centers. The question is still to distinguish of different types of  $\text{Cr}^{4+}$  centers (475 nm, 550 nm, 660 nm, 705 nm, 725 nm, 800 nm and 986 nm and assign them to concrete site in the  $\text{Mg}_2\text{SiO}_4:\text{Mg}$ , Cr lattice: tetrahedral  $\text{Si}^{4+}$  site (substitution of  $\text{Cr}^{4+}$ ,  $\text{Cr}^{5+}$  and  $\text{Cr}^{6+}$  ions), octahedral  $\text{Mg}^{2+}$  (4a) and  $\text{Mg}^{2+}$  (4c) sites (substitution of  $\text{Cr}^{3+}$  ions and  $\text{Cr}^{4+}$  ions).

Bearing in mind all the above results one can conclude that one of the method of improving of the emission features of  $\text{Cr}^{4+}$  centers in the  $\text{Mg}_2\text{SiO}_4:\text{Mg}$ , Cr single crystal is controlling of the initial Cr content in the melt and the oxygen partial pressure during the growth as it was stated in [7]. But formation of tetravalent  $\text{Cr}^{4+}$  ion being related to the  $\text{O}^{2-}$  vacancy existing in the crystal may be a critical factor. So, if conditions of optimal Cr doping content and optimal oxygen partial pressure can not be satisfied, one can deal with annealing in  $\text{O}_2$  to increase of  $\text{Cr}^{4+}$  emitting centers and, after that, with  $\gamma$ -irradiation of the crystal. The latter improves excitation conditions and emission characteristics, giving a crystal with higher amount of  $\text{Cr}^{4+}$  emitting centers. It may be due to also F-color centers (a band between 350 and 570 nm observed after  $\gamma$ -irradiation) which may participate in energy transfer of the excitation to  $\text{Cr}^{4+}$  giving rise in  $\text{Cr}^{4+}$  emission. Very similar effects were previously observed for YAG:Cr,Tm,Ho crystal for laser applications [10]. Due to recharging of Cr ions under influence of annealing in the air and subsequent  $\gamma$ -irradiation possible was the increase in a laser output efficiency of the crystal.

## 5 Conclusions

The formation of tetravalent Cr ions is related not only to the initial Cr content in the melt, oxygen partial pressure and  $\text{O}^{2-}$  vacancy existing in the crystal, but also to the external field such as  $\gamma$ -irradiation. The additional absorption after  $\gamma$ -irradiation show the decrease in intensity of the absorption of  $\text{Cr}^{3+}$  and  $\text{Cr}^{4+}$  ions in some part of the spectrum and increase in the other giving evidence on recharging effects between  $\text{Cr}^{3+}$  and  $\text{Cr}^{4+}$ . There arises also a color centers observed between 380 nm and 570 nm that may participate in energy transfer of any excitation to  $\text{Cr}^{4+}$  giving rise to  $\text{Cr}^{4+}$  emission. Opposite to forsterite crystal, absorption spectrum of YAG:Ca, Cr crystal after  $\gamma$ -irradiation reveals only increase in the absorption of the Cr bands. The observed behavior of the absorption spectrum of YAG:Ca, Cr crystal under influence of  $\gamma$ -irradiation suggests that  $\gamma$ -irradiation ionizes only Cr ions.

## References

- [1] V. Petricevic, S. K. Gayen, and R. R. Alfano, *Appl. Phys. Lett.* **53**, 2590 (1988).
- [2] H. R. Verdun, L. M. Thomas, D. R. Andrauskas, T. McCollum, and A. Pinto, *Appl. Phys. Lett.* **53**, 2593 (1988).
- [3] C. Chudoba, J. G. Fujimoto, E. P. Ippen, and H. A. Haus, *Optics Lett.* **26**, 292 (2001).
- [4] G. R. Boyer and G. Kononovitch, *Optics Comm.* **133**, 205 (1997).
- [5] Y. Yamaguchi, K. Yamagushi, and Y. Nobe, *J. Cryst. Growth* **128**, 996 (1993).
- [6] C. Jousseume, A. Kahn-Harari, D. Vivien, J. Derouet, F. Ribot, and F. Villain, *J. Mat. Chem.* **12**, 1525 (2002).
- [7] W. Chen and G. Boulon, *Opt. Mat.* **24**, 163 (2003).
- [8] S. Kück, U. Pohlmann, K. Petermann, G. Huber, T. Schönherr, *J. Lumin.* **60–61**, 192–196 (1994).
- [9] B. Henderson, H. G. Gallagher, T. P. J. Han, and M. A. Scott, *J. Phys.: Condens. Mat.* **12**, 1927 (2000).
- [10] S. M. Kaczmarek, W. Żendzian, T. Łukasiewicz, K. Stepka, Z. Moroz, and S. Warchoł, *Spectrochim. Acta A* **54**, 2109 (1998).
- [11] R. D. Shannon and C. T. Prewitt, *Acta Cryst.* **B 25**, 925 (1969).
- [12] R. Moncorgé, H. Manaa, and G. Boulon, *Opt. Mat.* **4**, 139 (1994).
- [13] M. Gaft, G. Boulon, G. Panczer, Y. Guyot, R. Reisfeld, S. Votyakov, G. Bulka, *J. Lumin.* **87–89**, 1118 (2000).
- [14] M. Hazenkamp and H. Gudel, *J. Lumin.* **69**, 235 (1996).
- [15] S. M. Kaczmarek, R. Jabłoński, I. Pracka, G. Boulon, T. Łukasiewicz, Z. Moroz, and S. Warchoł, *Nucl. Instr. Meth. B* **142**, 515 (1998).
- [16] I. Sh. Akhmadulin, S. A. Mihachev, and S. P. Mironov, *Nucl. Instr. Meth. B* **65**, 270 (1992).
- [17] S. M. Kaczmarek, M. Berkowski, Z. Moroz, and S. Warchoł, *Acta Phys. Pol. A* **96**, 417 (1999).